

## Symbols used

$B$	[-]	deformation factor
$c_L$	[eq(H <sup>+</sup> )/l]	H <sup>+</sup> ion exchange capacity related to catalyst volume
$c_t$	[mol/l]	total molar concentration
$D_{eff}$	[m <sup>2</sup> /s]	effective transport coefficient
$D^{G,L}$	[m <sup>2</sup> /s]	transport coefficient in gel phase or liquid phase
$\mathcal{D}_{ij}$	[m <sup>2</sup> /s]	binary Maxwell-Stefan diffusion coefficient of pair i-j
$m_1$	[-]	volumetric distribution ratio of component 1
$N$	[-]	number of components
$N_I$	[mol/(m <sup>2</sup> s)]	molar flux density of component 1
$q$	[g/g]	solvent loading of polymer
$R$	[J/(mol K)]	universal gas constant
$r$	[mol/(eq(H <sup>+</sup> ) s)]	intrinsic rate constant
$r_{eff}$	[mol/(eq(H <sup>+</sup> ) s)]	effective reaction rate
$S_V$	[m <sup>2</sup> /m <sup>3</sup> ]	specific external surface
$T$	[°C]	temperature
$x_i$	[-]	mole fraction of component i

## Greek symbols

$\varepsilon^M$	[m <sup>3</sup> /m <sup>3</sup> ]	relative volume of macropores
$\varepsilon^T$	[m <sup>3</sup> /m <sup>3</sup> ]	total porosity of support material
$\eta$	[-]	catalyst effectiveness factor
$\Phi$	[-]	Thiele modulus
$\varphi_p$	[-]	particle contact factor
$\mu_1$	[J/mol]	chemical potential of component 1
$\tau$	[-]	tortuosity factor

## Abbreviations

GFP	catalyst made by precipitation polymerization in a porous support
IB	isobutene
1B	1-butene
MeOH	methanol
MTBE	methyl- <i>t</i> -butylether

## Superscripts

b	bulk
G	gel phase
GL	gel phase and liquid phase in series
L	liquid phase

## References

- [1] German Patent 4,234,779.3 (1992) Inv: Hoffmann U.; Kunz U.; Bruderreck H.; Gottlieb K.; Schädlich K.; Becker S.

- [2] Kunz U.; Hoffmann U., *Preparation of Catalysts VI, Scientific Bases for the Preparation of Catalysts*, Elsevier Science 1995, pp. 299–308.  
 [3] Kunz U.; Künne H.; Hoffmann U., *Erdöl Erdgas Kohle 113* (1997) pp. 35–37.  
 [4] Zehner P.; Schlünder E.U., *Chem. Ing. Tech.* 42 (1970) pp. 933–941.  
 [5] Sundmacher K., *Reaktivdestillation mit katalytischen Füllkörperpackungen – ein neuer Prozeß zur Herstellung der Kraftstoffkomponente MTBE*, CUTEC-Schriftenreihe, Monographie Nr. 17, 1995, Clausthal-Zellerfeld (ISBN 3-930697-86-6).  
 [6] Taylor R.; Krishna R., *Multicomponent Mass Transfer*, John Wiley, New York 1993.  
 [7] Yasuda H.; Lamaze C. E.; Peterlin A.; *J. Pol. Sci.* 9 (1971) pp. 1117–1131.  
 [8] Künne H., *Reaktionstechnische Untersuchungen für einen neuen Katalysatortyp zur Flüssigphasensynthese des Antiklopffmittels MTBE*, Dissertation, TU Clausthal 1996.  
 [9] Rehfinger A.; Hoffmann U., *Chem. Eng. Sci.* 45 (1990) pp. 1605–1626.

*This paper was also published in German in Chem. Ing. Tech. 70 (1998) No. 3.*

## Investigation of the Reduction of Nitric Oxides by CO and H<sub>2</sub> on Pt-Mo Catalysts under Oxidizing Conditions

By Brigitta Frank, Ragnar Lübke, Gerhard Emig, and Albert Renken\*

### 1 Problem

In the mid 1980s the so-called three-way catalyst was introduced in Europe. It reduces the three components CO, H<sub>2</sub>, and NO<sub>x</sub> from automotive exhaust, if oxygen is introduced stoichiometrically to the motor ( $\lambda = 1 \pm 0.02$ ). Today, the additional concern about carbon dioxide emissions leads to the demand of lean-burn petrol engines. These engines work with an excess of O<sub>2</sub> ( $\lambda > 1$ ); thus, less fuel is needed and less CO<sub>2</sub> is produced. However, the exhaust gas of lean-burn petrol and diesel engines contains 5–11 Vol.-% O<sub>2</sub> [1]. As the currently used three-way catalyst in passenger cars is not able to reduce nitric oxides under oxidizing conditions, a new catalyst must be developed (DeNOx catalyst). Furthermore, the current three-way catalyst contains the scarce metal rhodium and many attempts are being made by the automotive industry to develop Rh-free catalysts [2].

In a preceding work [3] it was found that on Pt-Mo catalysts nitric oxides can be reduced by hydrogen in an excess of oxygen as present in the exhaust of power plants. Some features of the Pt-Mo catalyst (Rh-free, activity < 200 °C) makes it an interesting candidate for automotive exhaust control of lean-burn cars, where additionally small quantities of CO are present [1]. Lean-burn car exhaust contains considerably less CO than commonly used car exhaust does (up to 0.6% CO instead of 3% CO). However,

[\*] Dr.-Ing. B. Frank and Prof. Dr. A. Renken (albert.renken@epfl.ch), Institut de Génie Chimique, ETH Lausanne, CH-1015 Lausanne, Switzerland; Dipl.-Ing. R. Lübke und Prof. Dr.-Ing. G. Emig (emig@t-c.uni-erlangen.de), Lehrstuhl für Technische Chemie I, Universität Erlangen-Nürnberg, D-91058 Erlangen, Germany.

CO is still present and may significantly influence the reaction behavior.

Therefore, in the present study the NO<sub>x</sub> reduction by H<sub>2</sub> and CO in oxidizing atmospheres was studied, using Pt-Mo catalyst supported on α-Al<sub>2</sub>O<sub>3</sub>. The catalyst developed by Wildermann [3] was compared to three-component catalysts containing Pt-Mo and a third metal (Co, Cu or Ni).

## 2 Experimental

The experimental set-up consisted of three parts: gas supply, recycle loop reactor, and analysis part. Gases were supplied by mass flow controllers (Bronkhorst, NL). Gases (Carbagas, Lausanne) were used without further treatment.

The developed recycle-reactor with an external recycle loop and an overall volume of 480 ml is shown in Fig. 1. The reaction mixture flowed upward in the outer tube where it was heated preliminary and then downward in the inner tube passing the catalytic bed. This set-up allowed isothermal operation. A membrane compressor (KNF Neuberger, Glattbrugg) recycled the gas; the volumetric flow rate inside the recycle loop was measured by a mass flow meter. The recycle ratio (ratio of the volumetric flow rate inside the recycle loop to the volumetric flow rate at the outlet) was 50 for all experiments, the reactor can be modeled as an ideal continuous stirred tank reactor [5]. The reactor was heated by an oven in two parts (Vinci Technologies, Paris) and kept at the desired temperature by an external PID regulator (Eurotherm, Glattbrugg). The temperature inside the reactor was measured by a separate thermocouple movable within a glass capillary.

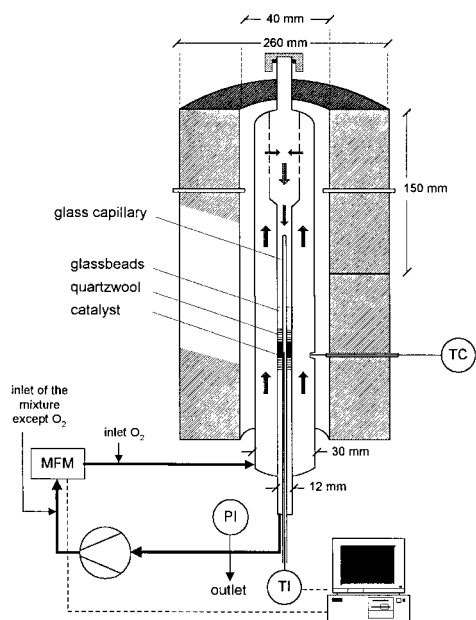


Figure 1. Recycle reactor used.

- As O<sub>2</sub> is introduced separately into the reactor (Figure 1), only NO and no NO<sub>2</sub> is present at the reactor inlet.

The reactor effluent was measured by two gas chromatographs, two infrared detectors for NO and CO<sub>2</sub> (Siemens), and a chemiluminescence analyzer for NO<sub>x</sub> (Thermo Environmental Instruments). One gas chromatograph with helium as the carrier gas was operated at 35 °C and analyzed for N<sub>2</sub> and CO (Porapak S, 4.6m, 1/8", 80/100 mesh and molecular sieve 5A, 4m, 1/4", 60/80 mesh). The second gas chromatograph with N<sub>2</sub> as the carrier gas analyzed for H<sub>2</sub>, N<sub>2</sub>O, and CO<sub>2</sub> (Porapak S and Q, 3m, 1/8", 80/100 mesh, 35–170 °C) [5]. The analysis times were 52 and 40 min, respectively. The installation was computer-controlled and measurements were taken continuously. The mass balance of N and C of each experimental point was controlled; it was within ±5%.

Different Pt-Mo catalysts (1–1.25 mm fraction) supported on α-Al<sub>2</sub>O<sub>3</sub> were used: 0.5% Pt – 3.4% Mo and 0.2% Pt – 0.7% Mo – 0.1% X (X = Co, Cu or Ni). All catalysts were prepared by a dry impregnation technique [3] and pretreated by oxidation in flowing O<sub>2</sub> (10 % in Ar) for 1.5 h at 400 °C, reduction by hydrogen (10% in Ar) for 2 h at 400 °C, and a subsequent conditioning for 12 h at 450 °C using a feed of 2% NO and 1% CO. The BET- surface of the support was below 3 m<sup>2</sup>/g and the mean pore diameter was 400 nm. External and internal heat or mass transfer limitations can be excluded under experimental conditions [5].

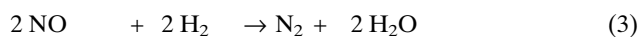
The conversions of NO<sub>x</sub>, CO or H<sub>2</sub> were calculated assuming a constant volume flow rate  $\dot{V}$  according to

$$X_i = \frac{y_{i,0} - y_i}{y_{i,0}} \quad i = \text{NO}_x, \text{CO or H}_2 \quad (\dot{V} = \text{const.}) \quad (1)$$

(y = mole fraction in the gas phase, index 0 = at the reactor inlet). The stoichiometric ratio  $\lambda$  at the inlet was calculated according to

$$\lambda = \frac{y_{\text{NO}} + 2y_{\text{O}_2}}{y_{\text{CO}} + y_{\text{H}_2}} \quad (2)$$

In the system NO/CO/H<sub>2</sub>/O<sub>2</sub> the reactions of Eqs.(3–9) may take place:



The formation of NH<sub>3</sub> can be excluded under oxidizing conditions as used in this work [3,4]. Experiments with a fixed-bed of glass beads showed that the homogeneous gas-phase oxidation of NO to NO<sub>2</sub> takes place and that 50% of the NO was converted to NO<sub>2</sub>. Nevertheless, in a first approximation NO and NO<sub>2</sub> have similar activities [5] and, therefore, in this study only the NO<sub>x</sub> concentration (NO + NO<sub>2</sub>) was considered.

### 3 Results and Discussion

#### 3.1 Influence of the NO Concentration

In Fig. 2 the dependence of the NO<sub>x</sub> and H<sub>2</sub> conversions upon the inlet NO mole fraction is depicted. Without NO the H<sub>2</sub>/O<sub>2</sub> reaction is nearly completed at temperatures as low as 70 °C (Eq. 7). At 0.1% NO the conversion of NO<sub>x</sub> starts to increase at 70 °C and passes through a broad maximum at 90–120 °C with 80% NO<sub>x</sub> conversion. With further increasing temperature the NO<sub>x</sub> conversion decreases to 16% at 200 °C. Obviously, at higher temperatures the O<sub>2</sub>/H<sub>2</sub> reaction (Eq. 7) occurs preferentially. With increasing NO concentrations, the maximum of NO<sub>x</sub> conversion decreases and is shifted to higher temperatures. This suggests that at these temperatures NO is strongly adsorbed at the surface inhibiting the reaction. This finding is in agreement with literature, where a negative order of NO is found [3]. The H<sub>2</sub> conversion increases gradually with increasing temperature until H<sub>2</sub> is completely converted. With increasing inlet mole fractions of NO, the H<sub>2</sub> conversion is shifted toward higher temperatures.

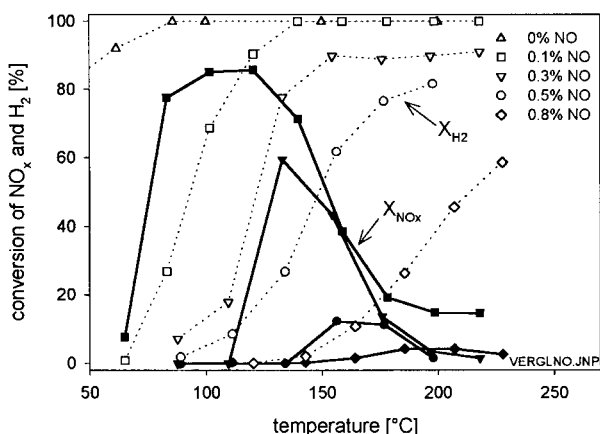


**Figure 2.** Influence of nitric oxide on the NO<sub>x</sub> and the H<sub>2</sub> conversion on a Pt-Mo catalyst using 0–0.8% NO, 0.8% H<sub>2</sub>, 8% O<sub>2</sub> (open symbols; X<sub>H<sub>2</sub></sub>, closed symbols; X<sub>NO<sub>x</sub></sub>).

#### 3.2 Catalyst Screening

The activity of the 0.5% Pt – 3.4% Mo catalyst is compared to the activity of three-component catalysts, containing 0.2% platinum, 0.7% molybdenum, and additionally 0.1% of a third component, i.e., copper, nickel or cobalt. The reaction conditions (constant volume flow rate of 150 Nml/min, recycle reactor) are chosen in a way that the quantities of platinum are comparable and, thus, the same conversion should be obtained [5].

The NO<sub>x</sub> conversion of all catalysts passes through a pronounced maximum with increasing temperature. In Fig. 3 the conversions of NO<sub>x</sub>, CO, and H<sub>2</sub> on the Pt-Mo catalyst and of freshly pretreated Pt-Mo-Co catalyst are plotted versus the temperature. On both catalysts the CO conversion starts to increase at the lowest temperature. For the Pt-Mo-Co catalyst the CO conversion is already completed as the

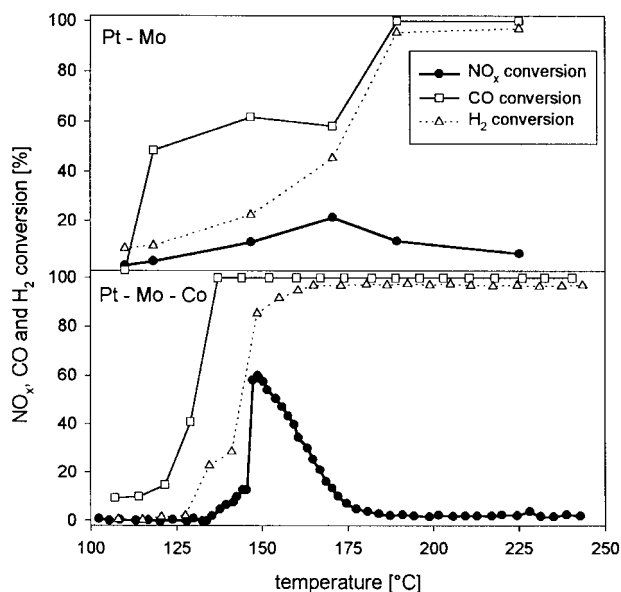


**Figure 3.** Temperature dependence of the NO<sub>x</sub>, CO, and H<sub>2</sub> conversions. Comparison of the Pt-Mo and a freshly pretreated Pt-Mo-Co catalyst (0.3% NO, 0.3% CO, 0.8% H<sub>2</sub>, 8% O<sub>2</sub>).

reduction of NO starts. This shows that CO does not participate in the NO<sub>x</sub> reduction and that reactions between NO and CO as proposed in the Eqs.(5) and (6) can be ruled out. The conversion of H<sub>2</sub> strongly increases with the sudden increase of the NO<sub>x</sub> conversion, indicating that hydrogen reduces NO<sub>x</sub>. However, at higher temperatures the reaction of H<sub>2</sub> with oxygen is favored compared to the reaction with NO<sub>x</sub> and consequently the NO<sub>x</sub> conversion decreases.

The CO conversion exhibits an interesting effect on the Pt-Mo catalyst. Although the CO conversion increases up to 150 °C, for further increasing temperatures the CO conversion decreases from 62% at 150 °C to 56% at 175 °C. The CO conversion is only completed at 184 °C as the reduction of NO attained its maximum. Similar tendencies are observed for the Pt-Mo-Ni catalyst (not shown). On this catalyst the NO<sub>x</sub> conversion decreases from 85% at 131 °C to 64% at 175 °C before being completed at 185 °C. This might be explained in terms of a competing adsorption of NO and CO. Since at higher temperatures the NO adsorption is favored to the CO adsorption [5], the CO conversion might decrease in a certain temperature range. Only as the reaction of NO<sub>x</sub> takes place can the CO conversion be fully completed.

The maximum values for the NO<sub>x</sub> conversions and corresponding temperatures of all catalysts are presented in the first two columns of Tab. 1. On the Pt-Mo catalyst the NO<sub>x</sub> conversion reaches a maximum value of 22% at approximately 170 °C. The NO<sub>x</sub> conversion of the three-component catalysts, likewise, passes through a maximum with increasing temperature differing solely in the maximum value of NO<sub>x</sub> conversion and in the temperature of the maximum. The nickel and the copper containing catalyst have NO conversions below 20% which is slightly less than the Pt-Mo catalyst. The cobalt containing catalyst has a

three-fold higher conversion of NO at the maximum (60%) than the Pt-Mo catalyst, and its maximum appears at the lowest temperature (149 °C). The activity of NO<sub>x</sub> reduction of the three-component catalysts increases in the following order: Cu < Ni << Co (Tab. 1). This reflects the NO dissociative adsorption ability of the three metals, which is the highest for Co [6].

**Table 1.** Maximum NO<sub>x</sub> conversions ( $X_{\text{NO}_x, \text{max}}$ ) and corresponding temperatures (T at  $X_{\text{NO}_x, \text{max}}$ ) or temperature at 100% H<sub>2</sub> conversion (T at  $X_{\text{H}_2, 100}$ ) or at 100% CO conversion (T at  $X_{\text{CO}, 100}$ ). Experimental conditions: 0.3% NO, 0.3% CO, 0.8% H<sub>2</sub>, 8% O<sub>2</sub>.

Catalyst	$X_{\text{NO}_x, \text{max}}$	T at $X_{\text{NO}_x, \text{max}}$	T at $X_{\text{H}_2, 100}$	T at $X_{\text{CO}, 100}$
Pt - Mo	22%	170°C	190°C	147 / 190°C <sup>a</sup>
Pt - Mo - Co	60%	149°C	165°C	137°C
Pt - Mo - Cu	16%	204°C	228°C	162°C
Pt - Mo - Ni	18%	185°C	190°C	131 / 185°C <sup>a</sup>

<sup>a</sup> The temperature of the first CO maximum as well as the temperature of 100% CO conversion are indicated.

Although cobalt containing catalysts are reported to have good activity for NO reduction [7], some authors observed a decrease of the catalyst activity with increasing quantities of Co [8]. According to Yao and Shelef the difference in activity of Co catalysts is a question of the placement of the cobalt ion in the oxygen grid [9]. They found conclusive evidence that a tetrahedrally coordinated Co ion as in the spinel CoAl<sub>2</sub>O<sub>4</sub> is catalytically inactive, whereas an octahedrally coordinated Co as in the spinels Co<sub>3</sub>O<sub>4</sub> and ZnCo<sub>2</sub>O<sub>4</sub> is very active. The promoting effect of Co found in the present work might, therefore, be a consequence of the corundum structure of  $\alpha$ -Al<sub>2</sub>O<sub>3</sub>, where the Co ions are placed in the more favorable octahedral sites.

In Tab. 1 the temperature of the maximum NO<sub>x</sub> conversion is compared to the temperature of 100% H<sub>2</sub> conversion (column 3) and to the temperature where the first maximum or 100% conversion of CO appears (column 4). On all catalysts the complete H<sub>2</sub> conversion is attained at the highest temperature. On the Pt-Mo-Co and the Pt-Mo-Cu catalyst, complete CO conversion (on the other catalysts the first maximum of CO conversion) is attained at the lowest temperature. On the basis of these results it can be concluded that the following reactions occur in the NO/CO/H<sub>2</sub>/O<sub>2</sub> system at increasing temperatures: CO/O<sub>2</sub> < NO/H<sub>2</sub> < H<sub>2</sub>/O<sub>2</sub>. This reaction order is exactly the opposite as compared to the order of the individual reactions where O<sub>2</sub>/H<sub>2</sub> < NO/H<sub>2</sub> < CO/O<sub>2</sub> < NO/CO [5]. Obviously, the NO/H<sub>2</sub> reaction (Eqs. 3 + 4) and the O<sub>2</sub>/H<sub>2</sub> reaction (Eq. 7) can only start when the predominating surface species CO<sub>ad</sub> is removed by oxygen.

### 3.3 Influence of the CO Concentration

In Fig. 4 the NO<sub>x</sub> conversions on the Pt-Mo and the Pt-Mo-Co catalyst are compared for different concentrations of CO. The maximum values of NO<sub>x</sub> conversion are about 60% for both catalysts when no CO is present. Upon introducing

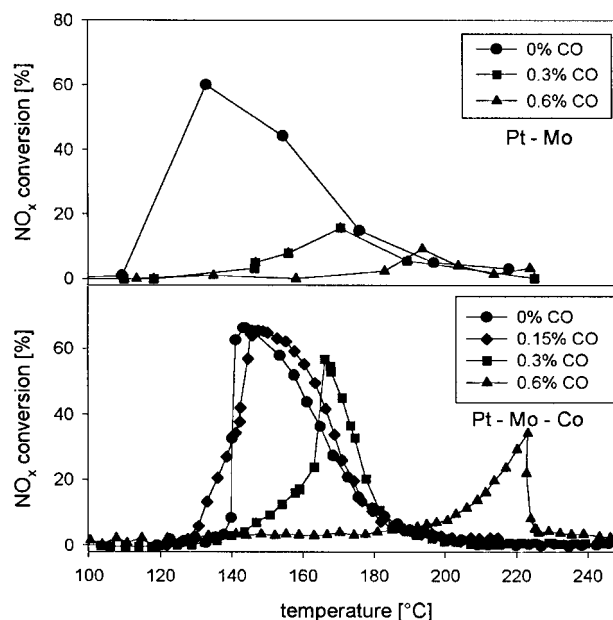


**Figure 4.** Comparison of the NO<sub>x</sub> conversion of the Pt-Mo and the Pt-Mo-Co catalyst (0.3% NO, 0.8% H<sub>2</sub>, 8% O<sub>2</sub>, 0–0.6% CO).

increasing quantities of CO the maximum value of NO<sub>x</sub> conversion decreases stronger for the Pt-Mo (to 10% at 0.6% CO) than for the Pt-Mo-Co catalyst (to 34% at 0.6% CO). These results reveal that in the presence of CO the Pt-Mo-Co catalyst has a higher activity of NO<sub>x</sub> reduction than the Pt-Mo catalyst.

## 4 Conclusions and Perspectives

In view of the increasing interest in reducing NO<sub>x</sub> in oxidizing atmospheres as present in the exhaust of diesel or lean-burn cars, the reduction of NO<sub>x</sub> by H<sub>2</sub> and CO was studied at 100–250 °C. The reduction of NO<sub>x</sub> by H<sub>2</sub> occurs on Pt-Mo catalysts at a high excess of O<sub>2</sub> ( $\lambda = 1$ –18). Under the conditions in the present study CO does not reduce NO<sub>x</sub> and inhibits the NO/H<sub>2</sub> as well as the O<sub>2</sub>/H<sub>2</sub> reaction. This is in agreement with literature findings [4,10]. In the present study the inhibiting effect of CO is found at the highest stoichiometric ratio of  $\lambda = 14$ –20 (comparison:  $\lambda = 0.8$ –3.5 [4]). Nevertheless, the addition of Co as a third catalyst component increases the NO<sub>x</sub> conversion significantly in the presence of 0.3–0.6% CO. Such CO concentrations correspond to CO concentrations in the exhaust of lean-burn cars [1]. These findings are promising for the future development of DeNO<sub>x</sub> catalysts for lean-burn cars.

## Acknowledgment

Financial support by the Swiss National Science Foundation is gratefully acknowledged.

Received: February 27, 1998 [K 2349]

## References

- [1] Bögner W.; Krämer M.; Krutzsch B.; Pischinger S.; Voigtländer D.; Wenninger G.; Wirbeleit F.; Brogan M. S.; Brisley R. J.; Webster D. E.; *Appl. Catal. B* 7 (1995) pp. 153–171.
- [2] Kreuzer T.; Lox E. S.; Lindner D.; Leyrer J.; *Catal. Today* 29 (1996) pp. 17–27.
- [3] Wildermann A.; *PhD work*, University of Erlangen-Nürnberg 1994.
- [4] Jones J. H.; Kummer J.T.; Otto K.; Shelef M.; Weaver E. E.; *Env. Sci. Technol.* 5 (1971) pp. 790–798.
- [5] Frank B.; *PhD work*, Swiss Federal Institute of Technology, Lausanne 1997.
- [6] Nieuwenhuys B. E.; in: *Elementary Reaction Steps in Heterogeneous Catalysis*, R. W. Joyer, R. A. v. Santen (Eds.) Kluwer Academic Publishers, Dordrecht 1993, pp. 155–177.
- [7] Armor J. N.; *Catal. Today* 26 (1995) pp. 147–158.
- [8] Yu Yao Y.-F.; *J. Catal.* 33 (1974) pp. 108–122.
- [9] Yao H. C.; Shelef M.; *J. Phys. Chem.* 78 (1974) pp. 2490–2496.
- [10] Gandhi H. S.; Yao H. C.; Stepien H. K.; in: *Catalysis under Transient Condition*, A. T. Bell, L. L. Hegedus (Eds.) ACS Symposium Series, Vol. 178, 1982, pp. 143–162.

This paper will also be published in German in *Chem. Ing. Tech.* 70 (1998) No. 7.

## Photochemical Treatment of Water: Comparison of Incoherent Excimer Lamps with a Medium-Pressure Mercury Lamp\*

By Thomas Oppenländer\*\*

### 1 Introduction

Incoherent excimer lamps [1] are used as radiation sources with outward or inward directed radiation geometry [2,3]. As a consequence of their variable geometry they may be used for photochemical processes of water treatment in immersion well reactors (IWR) or as flow-through reactors (FTR) (Fig. 1). In this context the Xe<sub>2</sub>\* and the KrCl\* excimer lamp are of strategic importance. They exhibit emission maxima at 172 nm (Vacuum-UV, VUV) or at 222 nm (UV-C), respectively. The UV-induced oxidative degradation of organic matter in water in the presence of hydrogen peroxide (H<sub>2</sub>O<sub>2</sub>-UV) or of ozone (O<sub>3</sub>-UV) is usually designated as *UV oxidation*. In contrast, the *VUV oxidation* is not dependent on the addition of supplementary oxidizing agents [4]. It is, however, of crucial importance for the further technical development of this innovative excimer lamp technology to economically compare their efficiency to that of conventionally applied medium-pressure mercury lamps.

[\*] Part of a paper presented at the GVC Annual Meeting, Sept. 24–26, 1997 in Dresden, Germany.

[\*\*] Prof. Dr. T. Oppenländer, Fachhochschule Furtwangen, University of Applied Sciences, Fachbereich Umwelt und Verfahrenstechnik, Jakob-Kienzle-Straße 17, D-78054 VS-Schwenningen, Germany.

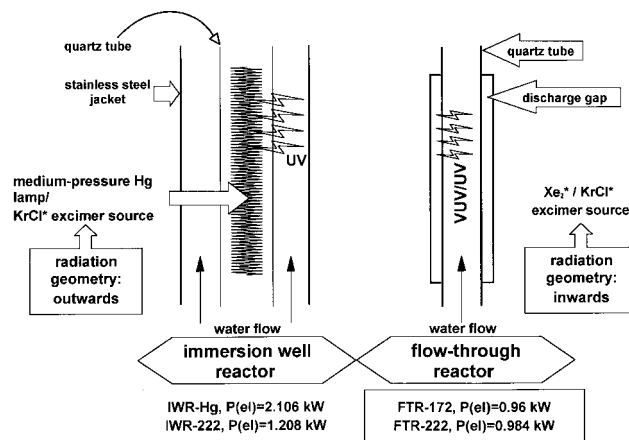


Figure 1. Schematic representation of the immersion well and flow-through photoreactors with the different geometries.

The aim of this study is, therefore, to compare a Xe<sub>2</sub>\* and a KrCl\* excimer source with a medium-pressure mercury lamp with respect to their efficiencies in photochemical water treatment on a phenomenological basis. Consequently, the medium-pressure Hg lamp is compared to the KrCl\* excimer lamp with outward directed radiation geometry within an immersion well photoreactor (annular photoreactors: IWR-Hg or IWR-222) and to the Xe<sub>2</sub>\* and KrCl\* excimer flow-through photoreactors that have inward directed radiation geometry (coaxial photoreactors: FTR-172 or FTR-222) (Fig. 1). Model waters were prepared by addition of the dyes Rhodamine B (RhB), Orange I, and Brilliant Blue (BB). The bleaching of these model waters by UV and VUV oxidation is usually described by pseudo first order kinetical treatment. The apparent rate constants will be compared based on the different lamp and photoreactor types and as a function of the water flow through the irradiation modules. Furthermore, the depletion of the total organic carbon content (TOC) of a solution of 2,4-dichlorophenol (2,4-DCP) in water by photomineralization within the four photoreactor types will be investigated.

Fig. 2 shows the emission spectra of the lamps which were used in this study. Whereas the novel excimer lamps exhibit narrow band and almost monochromatic emissions, the light output of the medium-pressure Hg lamp is of polychromatic

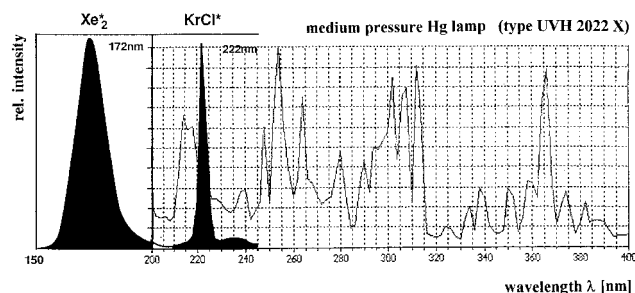


Figure 2. Comparison of the emission spectra of strategic important excimer lamps with the line spectrum of the medium-pressure mercury lamp.